# Small Oligomeric Micelles Based on End Group Modified mPEG−Oligocaprolactone with Monodisperse Hydrophobic Blocks

**Myrra G. Carstens,[†,‡] Jan J. L. Bevernage,[†] Cornelus F. van Nostrum,[†] Mies J. van Steenbergen,[†] Frits M. Flesch,[†] Ruud Verrijk,[‡] Leo G. J. de Leede,[‡] Daan J. A. Crommelin,[†] and Wim E. Hennink*[,†]**

*Department of Pharmaceutics, Utrecht Institute for Pharmaceutical Sciences (UIPS), Faculty of Pharmaceutical Sciences, Utrecht University, P.O. Box 80.082, 3508 TB Utrecht, The Netherlands, and OctoPlus N.V., Leiden, The Netherlands*

*Received August 27, 2006; Revised Manuscript Received October 17, 2006*

ABSTRACT: To design stable biodegradable micelles with a size smaller than 20 nm, the self-assembly of methoxypoly(ethylene glycol)-*b*-oligocaprolactones (mPEG-*b*-OCLs), and the effect of OCL block length and terminal derivatization with an aromatic group were studied. The studied oligomers consisted of an mPEG block with a molecular weight of 750 Da and a monodisperse OCL block of 1−7 units with a hydroxyl end group that was either unmodified, benzoylated or naphthoylated. They were prepared by preparative HPLC of the polydisperse block oligomers. Differential scanning calorimetry demonstrated that the two blocks were phase separated and crystallized separately. These block oligomers formed small and almost monodisperse oligomeric micelles with a hydrodynamic diameter of 8−15 nm, which could be tailored by the size of the hydrophobic block. The critical aggregation concentration (CAC) of the unmodified mPEG-*b*-OCLs was 0.03−4 mg/mL, and it decreased with increasing length of the OCL chain. End group modification resulted in an extensive reduction of the CAC to values as low as 0.003 mg/mL. This is expected to result in a better stability of these oligomeric micelles toward dilution upon intravenous administration, which makes these modified mPEG-*b*-OCLs very promising candidates for drug delivery purposes.

## Introduction

Polymeric micelles are nanoparticles with a core−shell structure that are formed by the self-assembly of amphiphilic block copolymers in water. They have interesting properties for a number of applications, in particular for drug delivery.[1−4] Generally, polymeric micelles have a size of 10−100 nm and their hydrophobic core can accommodate hydrophobic drugs, such as several anticancer agents.[1−4] Their small size and hydrophilic surface reduce uptake by the reticuloendothelial system (RES), resulting in long circulation times after intravenous injection. Consequently, polymeric micelles can extravasate and accumulate at tumors and other pathological sites, through the so-called enhanced permeability and retention (EPR) effect.[5] Poly(ethylene glycol)-*b*-polyesters are attractive and frequently studied polymers for the design of polymeric micelles. In particular polyesters such as poly(lactic acid) (PLA) and poly(ϵ-caprolactone) (PCL), have been used as the hydrophobic block of the amphiphilic polymers, because of their biodegradability and biocompatibility.[6−8] Poly(ethylene glycol) (PEG) is the most frequently used hydrophilic block, because of its low toxicity and "stealth" properties.[9−11] The self-assembly of PEG-*b*-polyesters, as well as loading of several types of hydrophobic drugs, have been extensively studied in recent years.[12−20] These studies mainly focused on high molecular weight block copolymers, which form micelles with a diameter greater than 30 nm. Micelles with a smaller size however benefit more from the EPR effect,[21] because of their longer circulation times and better tissue penetration, as demonstrated for shell cross-linked poly(*tert*-butyl acrylate)-*b*-poly(methyl acrylate) (PBA-*b*-PMA) and PBA-*b*-polystyrene (PBA-*b*-PS) nanoparticles.[22] Moreover, PEG5000-distearoylphosphatidyl ethanolamine (PEG-DSPE) micelles of 15 nm showed superior tumor accumulation when compared to 100 nm liposomes, after intravenous administration to mice with a subcutaneously established Lewis lung carcinoma.[23] Considering the end-to-end distance of the block copolymers in relation to the required micellar size, the formation of small micelles necessitates the use of low molecular weight block oligomers, such as the biodegradable mPEG-*b*-oligocaprolactones (mPEG-*b*-OCL), as studied in this publication. It is anticipated that the micellar size will depend on the size of the hydrophobic block and, consequently, that the use of monodisperse hydrophobic blocks will result in better size control of the micelles.

Besides size, the stability of a polymeric micelle is a key factor for its efficacy as drug delivery system. In order to achieve long circulation times and to obtain accumulation at the target site, the micelle should remain intact in vivo. However, destabilization of polymeric micelles may already occur upon injection into the bloodstream, since dilution may result in polymer concentrations below the critical aggregation concentration (CAC). This likely explains the limited number of reports on stable sub-20-nm nanoparticles, because the high CAC is inherent to the low molecular weight of the block oligomers forming these small micelles. Several strategies have been proposed to improve the micellar stability, including covalent[24−26] and physical[4,25] cross-linking of the micellar core or shell, as well as modification of the polymers to reduce their CAC.[4,27−30] The covalent cross-linking approach has been successfully applied by Shuai et al. to stabilize PEG-*b*-PCL micelles[26] and by Sun et al. to prepare the before mentioned small PBA-*b*-PMA and PBA-*b*-PS nanoparticles.[22] This strategy, however, carries the risk that the cross-linking procedure causes changes

* To whom correspondence should be addressed. Telephone: +31-30-2536964. Fax: +31-30-2517839. E-mail: W.E.Hennink@pharm.uu.nl.
† Department of Pharmaceutics, Utrecht Institute for Pharmaceutical Sciences (UIPS), Utrecht University.
‡ OctoPlus N.V., Leiden.

10.1021/ma0619738 CCC: $37.00 
Published on Web 12/14/2006

**Scheme 1. Synthesis of MEE- and mPEG-*b*-oligocaprolactone (a) and Modification of the Hydroxyl Group by Benzoylation (b1) or Naphthoylation (b2)**

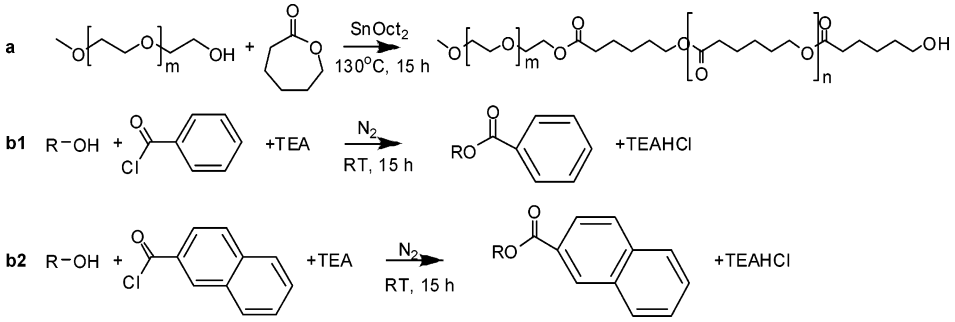


in the degradability of the block copolymer, as well as in the structural integrity of the loaded drug. Improved micellar stability has also been achieved by physical interactions between the amphiphilic block copolymers or with the encapsulated drug, for example by ionic interactions,[31] hydrogen bonding,[32] or stereocomplex formation.[33] The third strategy, reducing the polymer CAC by chemical modification of the hydrophobic block,[4,27−30] is followed in the present study.

Here, we use mPEG-*b*-OCL with monodisperse hydrophobic blocks. This approach allows a detailed study of the effect of the block oligomer composition for the design of stable sub-20-nm micelles. We demonstrate that terminal derivatization of mPEG-*b*-OCL with a benzoyl or naphthoyl group greatly improves its self-assembling properties, with regard to their future application in vivo.

## Experimental Section

**Materials.** Poly(ethylene glycol) mono(methyl ether) with a molecular weight of 750 Da and an $M_w/M_n$ of 1.05 (methoxyPEG, mPEG750), $\epsilon$-caprolactone (99%) and toluene were obtained from Acros Organics. Stannous octoate (tin(II) bis(2-ethylhexanoate), $SnOct_2$, >95%), 2-(2-methoxyethoxy)ethanol (MEE, 99%), benzoyl chloride (99%), 2-naphthoyl chloride (98%), chloroform-*d* ($CDCl_3$, 99.8% D), and 8-anilino-1-naphthalenesulfonic acid magnesium salt (1,8-ANS) were purchased from Sigma Aldrich Chemie BV and dichloromethane (DCM, peptide synthesis grade), acetonitrile (ACN, HPLC gradient grade), chloroform ($CHCl_3$, HPLC grade), and *N*,*N*-dimethylformamide (DMF, peptide synthesis grade) from Biosolve Ltd. Acetone, triethylamine (TEA, >99%), and ammonium acetate were obtained from Merck, pyrene from Fluka Chemie AG, magnesium sulfate exsiccatus from Bufa BV, and phosphate buffered saline (PBS, pH 7.4) from Braun. All chemicals were used as received; buffers were filtered through a 20 nm filter (Anotop, Whatmann) prior to use.

**Synthesis, End Group Modification, and Fractionation of Poly(ethylene glycol)-*b*-oligocaprolactone.** Poly(ethylene glycol)-*b*-oligocaprolactones (mPEG-*b*-OCLs) were synthesized by ring-opening polymerization of $\epsilon$-caprolactone, initiated by mPEG750, and catalyzed by $SnOct_2$ (Scheme 1a).[7,16,34] In detail, $\epsilon$-caprolactone (20 g) and mPEG750 in a molar ratio of 4/1 were heated to 130 °C. $SnOct_2$ (0.05 equiv) dissolved in 1 mL of toluene was added and the mixture was stirred overnight at 130 °C and cooled down to room temperature. To yield benzoylated and naphthoylated mPEG-*b*-OCL, the hydroxyl end group of mPEG750-*b*-OCL was reacted with benzoyl chloride or 2-naphthoyl chloride, respectively, as follows (Scheme 1b): A 20 g sample of mPEG750-*b*-OCL was dissolved in 20 mL of dry DCM with a 5-fold excess of TEA. This solution was added dropwise to a solution of 5 equiv of either benzoyl chloride or 2-naphthoyl chloride in 20 mL of dry DCM and stirred overnight under nitrogen atmosphere. Finally, the solvent was removed under reduced pressure.

The polydisperse oligomers were fractionated by preparative reversed phase HPLC (RP−HPLC), as reported previously for mPEG-*b*-oligolactates[35] with slight adaptations. The system consisted of a Waters 600EF Quaternary gradient pump and a Waters 2700 sample manager. A 5 mL aliquot of a 10% (w/w) solution of polydisperse block oligomer in acetonitrile/1 M ammonium acetate buffer pH 5 40/60 w/w was injected onto the column (Waters Xterra Prep MS C18 10 $\mu$m, 19 × 250 mm, including a guard column). A gradient was run from 70% A (water/acetonitrile 95/5 w/w) to 100% B (acetonitrile/water 95/5 w/w) in 30 min and from 60% A to 100% B in 25 min for the unmodified and the modified oligomers, respectively. The flow rate was 17 mL/min, and the detection wavelengths were 195 and 210 nm, respectively. Fractions were collected, and after evaporation of the solvents the products were characterized.

To investigate the thermal behavior (vide infra) of the hydrophobic block separately, 2-(2-methoxyethoxy)ethanol (MEE)-OCL was synthesized and fractionated as well, using the same procedure as for the synthesis and fractionation of mPEG750-*b*-OCL.

**Characterization of the Block Oligomers.** The purity of the fractions was assessed by analytical RP−HPLC, using a model 2695 Alliance (consisting of a pump, autosampler and injector), and a model 2487 absorbance meter (Waters). A 50 $\mu$L aliquot of a solution of 10 mg/mL in a mixture of 50/50 w/w acetonitrile/10 mM ammonium acetate buffer pH 5 was injected onto the column (Waters XTerra MS C18 (5 $\mu$m, 4.6 × 250 mm) including a guard column). A gradient was run from 100% A ($H_2O$/ACN 95/5 w/w) to 100% B ($H_2O$/ACN 5/95 w/w) in 30 min at a flow rate of 1 mL/min. Peaks were detected by UV ($\lambda$ = 210 nm). The chromatograms were analyzed using Empower software (Empower Pro, Waters corporation).

Electrospray mass spectrometry of oligomer samples of 0.1 mg/mL in 50/50 v/v acetonitrile/10 mM ammonium acetate buffer pH 5 was performed using a Shimadzu LCMS QP8000. The cone voltage was +4.5 kV with a detector voltage of 1.5 kV. The CDL voltage was set at −10 V, the CDL temperature was 250 °C, and the deflector voltage was 80 V. The flow of the nebulizing gas ($N_2$) was 4.5 L/min. Instrumental control was performed with a CLASS 8000 LCMS Software Package.

$^1$H NMR spectra were recorded using a Gemini spectrometer (Varian Associates Inc. NMR Instruments, Palo Alto, CA) operating at 300 MHz with $CDCl_3$ as a solvent. As reference line the chloroform peak at 7.24 ppm was used. Chemical shifts of MEE- and mPEG-*b*-OCL ($\delta$, ppm): 4.19 (t, 2H, O−$CH_2$−$CH_2$−O−CO), 4.03 (t, 2H, $CH_2$−$CH_2$−$CH_2$−O−CO), 3.67−3.50 (m, O−$CH_2$−$CH_2$−O; $CH_2$−OH), 3.35 (s, 3H, O−$CH_3$), 2.33−2.27 (m, CO−$CH_2$−$CH_2$−$CH_2$), 1.64−1.53 (m, CO−$CH_2$−$CH_2$−$CH_2$−$CH_2$−$CH_2$−$CH_2$−O), 1.37 (q, CO−$CH_2$−$CH_2$−$CH_2$−$CH_2$−$CH_2$−O). Chemical shifts of the benzoyl end group ($\delta$, ppm): 8.0 (d, 2H, aromatic CH), 7.53 (t, 1H, aromatic CH), 7.41 (t, 2H, aromatic CH), 4.29 (t, 2H, $CH_2$−O−CO−($C_6H_5$)). Chemical shifts of the naphthoyl end group ($\delta$, ppm): 8.57 (s, 1H, aromatic CH), 8.02 (d, 1H, aromatic CH), 7.94 (d, 1H, aromatic CH), 7.86 (d, 2H, aromatic CH), 7.54 (m, 2H, aromatic CH), 4.29 (t, 2H, $CH_2$−O−CO−($C_{10}H_7$)).

Both fractionated and polydisperse oligomers were characterized by gel permeation chromatography (GPC), using a PLgel OligoPore column (300 × 7.5 mm, including a Guard column, 50 × 7.5 mm)

(Polymer Laboratories) and low molecular weight PEG standards. The system used consists of a model 2695 Alliance, and a model 2142 RI-detector (Waters). The eluens was $CHCl_3$ at an elution rate of 1 mL/min and a temperature of 40 °C. This method was also used to determine the recovery of block oligomer after the particle formation process (vide infra). In detail, one mL of filtered and non-filtered particle dispersion of 10 mg/mL in 150 mM ammonium acetate solution (pH 6.8) was freeze-dried and the residue was dissolved in 3 mL of $CHCl_3$. The concentration was determined by GPC and compared with the amount of material used for the film formation. A linear relationship between the peak area and the concentration was shown in a concentration range of 1−5 mg of oligomer/mL of $CHCl_3$.

The melting temperature ($T_m$) of the fractionated MEE- and mPEG-*b*-oligocaprolactones was determined by differential scanning calorimetry (DSC), using a Q1000 differential scanning calorimeter (TA Instruments). Calibration of temperature and heat flow was performed with indium. Samples of approximately 5 mg in hermetically closed aluminum pans were subjected to a heat-cool-heat program from −80 to +100 °C at a heating rate of 10 °C/min and a cooling rate of 2 °C/min. Triplicate measurements were performed.

**Determination of the Critical Aggregation Concentration.** For the determination of the critical aggregation concentration (CAC) of the various block oligomers, two methods were used, each with a different fluorescent probe, pyrene and 8-anilino-1-naphthalenesulfonic acid magnesium salt (1,8-ANS), respectively. The fluorescence of pyrene as a function of different concentrations of block oligomer in phosphate buffered saline (PBS) was measured as described previously.[35,36] Briefly, samples were prepared in PBS at concentrations ranging from 0.0005 to 10 mg/mL, to which a pyrene solution in acetone was added (end concentration $6.0 \times 10^{-7}$ M). Excitation spectra of pyrene were recorded from 300 to 360 nm at an emission wavelength ($\lambda_{em}$) of 390 nm using a Horiba Fluorolog fluorimeter at a 90° angle. The intensity ratio $I_{338}/I_{333}$ was plotted against the oligomer concentration to determine the CAC. 1,8-ANS was used according to a modified literature procedure.[37−40] In detail, block oligomer samples were prepared in PBS at concentrations ranging from 0.001 to 10 mg/mL. In a black 96 well plate (Greiner), 1 $\mu$L of a 5 mM 1,8-ANS-solution in DMF/$H_2O$ (1/10 v/v) was added to 100 $\mu$L of an oligomer dispersion in PBS. Fluorescence was measured using a FluoSTAR OPTIMA fluorimeter; the excitation wavelength ($\lambda_{ex}$) was 355 nm, and $\lambda_{em}$ was 520 nm. Since 1,8-ANS only has fluorescent properties in hydrophobic environment, the CAC was determined by plotting the fluorescence intensity vs the concentration. As a control, the fluorescence of the samples was measured before the addition of the 1,8-ANS solution.

**Particle Formation and Characterization.** Block oligomer dispersions were formed by hydration of an oligomer film, coated on the inside wall of a round bottomed flask by solvent evaporation of an oligomer solution in dichloromethane. The resulting dispersion had a concentration of 10 mg/mL in phosphate buffered saline (PBS), and was filtered through a 0.2 $\mu$m Anotop filter.

The size of the particles and their size distribution was measured by dynamic light scattering (DLS) using a Malvern CGS-3 multiangle goniometer (Malvern Ltd,. Malvern, U.K.), consisting of a HeNe laser source ($\lambda$ = 632.8 nm, 22 mW output power), temperature controller (Julabo water bath) and a digital correlator ALV-5000/EPP. Time correlation functions were analyzed using the ALV-60 × 0 Software V.3.X provided by Malvern, to obtain the hydrodynamic diameter of the particles ($Z_{ave}$) and the particle size distribution (polydispersity index, PDI). The samples were analyzed at 25 and 37 °C, both directly after preparation and after incubation at room temperature or 37 °C for several days.

Cryogenic transmission electron microscopy (Cryo-TEM) analysis was performed using a Tecnai12 transmission electron microscope (Philips) operating at 120 kV, with the specimen at −180 °C and under low-dose imaging conditions. Samples were prepared in a temperature and humidity-controlled chamber, using a "Vitrobot" . A thin aqueous film of oligomer dispersion was formed by blotting a 200 mesh copper grid covered with Quantifoil holey carbon foil (Micro Tools GmbH, Germany) at 25 °C and at 100% relative humidity (glow discharged grid; 1 blot during 0.5 s). The thin film was rapidly vitrified by quickly plunging the grid into liquid ethane and transferred into the microscope chamber using a GATAN 626 cryo-holder system. Images were recorded on a TemCam-0124 camera and processed with AnalySIS software.

**Determination of the Temperature Sensitivity.** The temperature sensitivity of the different oligomers was determined by static light scattering using a Horiba Fluorolog fluorimeter (650 nm, 90° angle).[35,36] Oligomer dispersions in PBS at a concentration of 10 mg/mL were heated from 0 to 75 °C at 1 °C/min, and scattering intensities were measured at 0.3 °C intervals.

## Results and Discussion

**Preparation and Characterization of Unmodified and Modified mPEG-*b*-oligocaprolactones.** Fractionation of the synthesized polydisperse mPEG-*b*-OCL with three different end

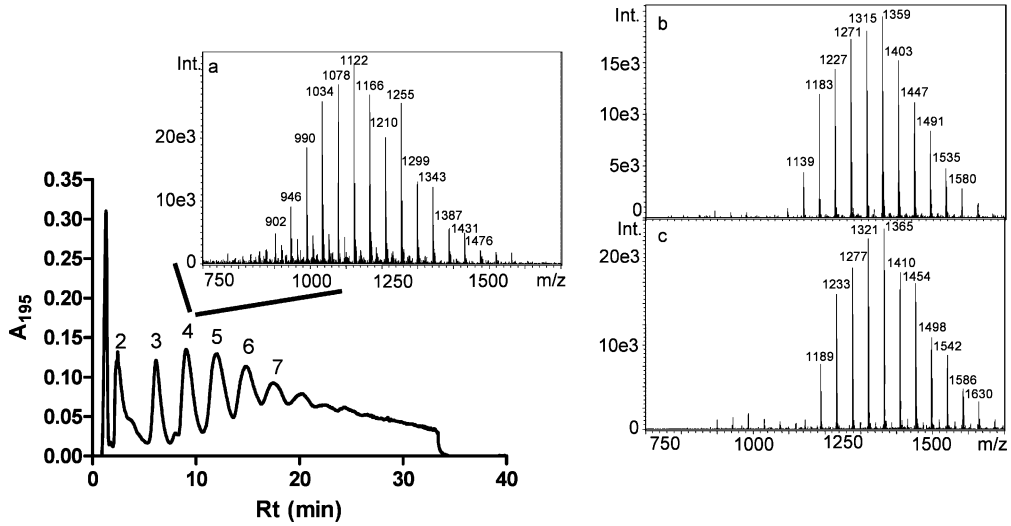


**Figure 1.** Preparative HPLC chromatogram of polydisperse mPEG750-*b*-OCL. The numbers represent the degrees of polymerization (DP) of the OCL block. The inset shows the mass spectrum of mPEG750-*b*-$OCL_4$ (a) and the spectra of benzoylated mPEG750-*b*-$OCL_4$ (b) and naphthoylated mPEG750-*b*-$OCL_4$ (c). Mass spectra show the ammonium adduct of the product, with a polydisperse PEG-block and a monodisperse OCL-block, as reflected by the PEG-distribution.

**Table 1. Molecular Weights (in kDa) of the Fractionated and Polydisperse Block Oligomers**

| | mPEG750-*b*-OCL$_x$ | | | | benzoylated mPEG750-*b*-OCL$_x$ | | | | naphthoylated mPEG750-*b*-OCL$_x$ | | | |
|---|---|---|---|---|---|---|---|---|---|---|---|---|
| *X* | $M_n$(Th)[a] | $M_n$(NMR)[b] | $M_n$(GPC) | $M_w/M_n$ | $M_n$(Th)[a] | $M_n$(NMR)[b] | $M_n$(GPC) | $M_w/M_n$ | $M_n$(Th)[a] | $M_n$(NMR)[b] | $M_n$(GPC) | $M_w/M_n$ |
| poly[c] | 1.20 | 1.23 | 1.28 | 1.15 | 1.31 | 1.35 | 1.05 | 1.33 | 1.36 | 1.31 | 1.23 | 1.20 |
| 1 | NA[d] | | | | 0.97 | 0.98 | 0.95 | 1.06 | 1.02 | 0.97 | 1.06 | 1.04 |
| 2 | 0.98 | 1.13 | 0.98 | 1.06 | 1.08 | 1.16 | 1.18 | 1.03 | 1.13 | 1.13 | 1.14 | 1.05 |
| 3 | 1.09 | 1.27 | 1.13 | 1.05 | 1.20 | 1.18 | 1.26 | 1.04 | 1.25 | 1.27 | 1.27 | 1.05 |
| 4 | 1.20 | 1.42 | 1.28 | 1.05 | 1.31 | 1.28 | 1.38 | 1.04 | 1.36 | 1.39 | 1.39 | 1.05 |
| 5 | 1.32 | 1.50 | 1.38 | 1.07 | 1.42 | 1.41 | 1.51 | 1.04 | 1.47 | 1.47 | 1.53 | 1.06 |
| 6 | 1.43 | 1.57 | 1.50 | 1.06 | 1.54 | 1.42 | 1.64 | 1.04 | 1.59 | 1.74 | 1.78 | 1.05 |
| 7 | 1.55 | 1.77 | 1.63 | 1.06 | 1.65 | 1.55 | 1.77 | 1.04 | NA[d] | | | |

[a] Theoretical value of the molecular weight, calculated from molecular weight of the mPEG block as provided by the supplier (750 Da), of the OCL block using the M/I ratio or the DP determined by ESI-MS (DP × 114) and of the end group (H = 1, benzoyl = 105, and naphthoyl = 155). [b] Calculated from $^1$H NMR in deuterated chloroform, from the signal ratio of the methylene protons of the OCL block and the PEG block to the protons of the methoxy group. [c] Polydisperse block oligomer, mPEG750-*b*-OCL, synthesized with a molar ratio of mPEG750/caprolactone of 1/4. [d] NA = Not available.

groups (the unmodified hydroxyl group, and its benzoyl and naphthoyl derivative) yielded a series of block oligomers with monodisperse hydrophobic blocks. In the mass spectra of each fraction, a regular series of peaks was observed, with a repeating unit of 44 Da, corresponding to one ethylene glycol unit (Figure 1). This indicates the presence of an oligomer with a polydisperse PEG block and a discrete OCL chain length. GPC demonstrated a decrease in the $M_w/M_n$ upon fractionation (Table 1). The $M_w/M_n$ was still slightly higher than one, due to the polydispersity of the PEG-block. The molecular weight values calculated from $^1$H NMR and the values obtained with GPC correlate well with the values calculated from the degree of polymerization (DP) of the OCL block determined by ESI−MS (Table 1). With analytical reversed phase HPLC it was found that the purity of the fractions was higher than 90%, except for the fractions with the highest DP: benzoylated mPEG-*b*-OCL$_7$ was contaminated with some DP 6, and naphthoylated mPEG-*b*-OCL$_6$ contained DP 7.

Differential scanning calorimetry (DSC) showed a clear melting endotherm in the thermograms of the fractionated MEE−OCL when the DP is 3 or higher (Figure 2a). The melting temperature ($T_m$) increased with the OCL chain length, from −25 to +31 °C for DP 3 to 7. This trend has also been observed for polydisperse OCL: melting temperatures of 31, 46, and 50 °C were reported for OCLs with average DPs of 5, 10, and 18, respectively.[41] The higher $T_m$ of polydisperse OCLs compared to monodisperse OCLs can be ascribed to the presence of longer chains in the polydisperse oligomer. In the thermograms of mPEG750-*b*-OCL$_{2\ and\ 3}$ melting endotherms were observed at 25 and 23 °C, respectively (Figure 2b). These are likely caused by the crystallization of the mPEG-block, since the thermograms of MEE−OCL did not show any endotherms at these temperatures. The observed $T_m$'s and $\Delta H$'s (147 and 135 J/g, respectively, corrected for the weight fraction of OCL) are slightly lower than those of mPEG750 (30 °C, 161 J/g), likely due to imperfections in the crystallization of mPEG-*b*-OCL block oligomers.[42,43] This may also explain the peak at −5 °C in the thermogram of mPEG750-*b*-OCL$_4$, which can be considered a sub-endotherm of the melting peak of the mPEG block. MPEG750-*b*-OCL$_4$ showed another endotherm at −25 °C, representing the melting of the OCL block. This $T_m$ and the $\Delta H$ (32 J/g, corrected for the weight fraction of PEG) are lower than those of MEE−OCL$_4$ (−1 °C and 85 J/g, respectively), most likely due to imperfect crystallization as well. At higher DPs, the melting endotherm of the OCL block shifts to higher temperatures and overlaps with the melting peak of mPEG750. The DSC data demonstrate that the two blocks of mPEG-*b*-OCL are phase separated and crystallize separately. Phase separation was also observed in polydisperse PEG−OCL triblock oligomers,[43] and in high molecular weight PEG-*b*-PCL

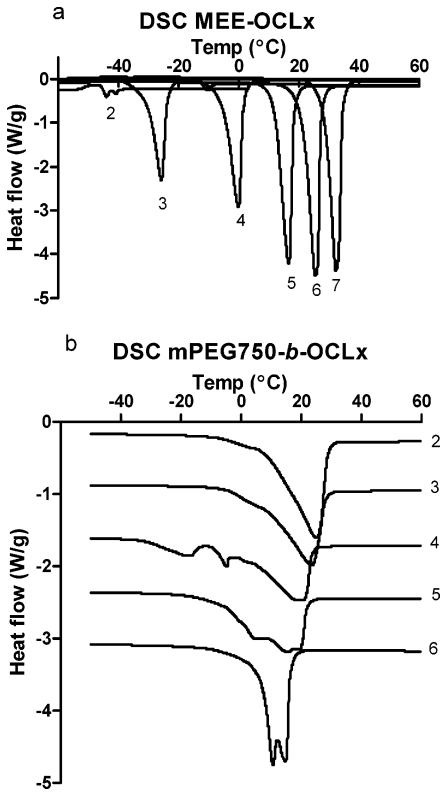


**Figure 2.** Thermograms of fractionated MEE-*b*-OCL (a) and mPEG750-*b*-OCL (b). Data of the second heating cycle are presented. Numbers represent the degrees of polymerization (DP) of the OCL block.

block copolymers.[42,44,45] Modification of the hydroxyl end groups of mPEG-*b*-OCLs with benzoyl or naphthoyl hardly affected the thermal behavior of the block oligomers (results not shown). Previously, it was shown that the two blocks of mPEG-*b*-oligolactate did not phase separate, which resulted in the formation of hydrated nanoparticles with a size around 400 nm upon self-assembly in water.[35] It is anticipated that phase separation of the two blocks of mPEG-*b*-OCL will favor the formation of more compact core−shell structures in water.

**The Effect of End Group Modification on the Critical Aggregation Concentration.** The critical aggregation concentration (CAC) of the various block oligomers was determined with two different fluorescent probes. In general, the CAC values obtained with 1,8-ANS are higher than those obtained with pyrene (Table 2). A difference between fluorescent probes has been observed previously, and may be explained by differences in interactions between the amphiphile and the probe.[37,40] As expected, the CAC decreased with increasing chain length of the hydrophobic block (>10 to 0.09 mg/mL determined with

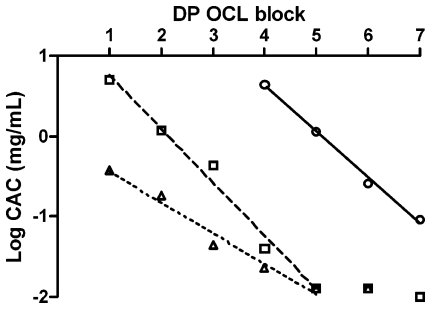


**Figure 3.** Critical aggregation concentration of mPEG750-*b*-$OCL_x$ (circles, straight line), benzoylated mPEG750-*b*-$OCL_x$ (squares, dashed line) and naphthoylated mPEG750-*b*-$OCL_x$ (triangles, dotted line) in phosphate buffered saline, determined with 1,8-ANS. Note: the data points of benzoylated and naphthoylated mPEG750-*b*-$OCL_{5 \text{ and } 6}$ overlap.

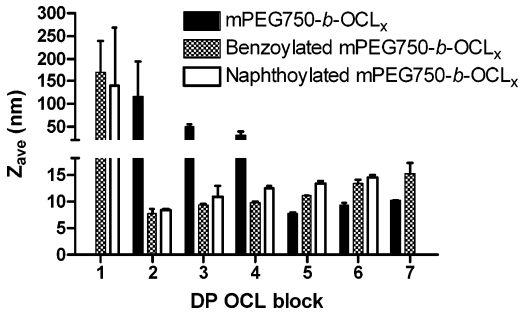


**Figure 4.** Hydrodynamic diameter ($Z_{ave}$) of (modified) mPEG750-*b*-$OCL_x$ in phosphate buffered saline (10 mg/mL), determined by dynamic light scattering. Mean ± SD of three individual preparations.

1,8-ANS for mPEG750-*b*-$OCL_{2 \text{ to } 7}$, Table 2), and a linear relationship was observed between the DP of the OCL block and the logarithm of the CAC of the block oligomers (Figure 3). Such a correlation was also observed in other homologous series of amphiphiles.[46] The CACs of the unmodified block oligomers are 2 orders of magnitude higher than those reported for high molecular weight PEG-*b*-PCL block copolymers,[18,19] and are also higher than those for low molecular weight but polydisperse mPEG750-*b*-OCL.[34] The latter is ascribed to the presence of longer chains in the polydisperse oligomer mixture, as compared to the fractionated oligomers studied in this paper. Interestingly, esterification of the hydroxyl end group of the block oligomer with an aromatic group dramatically decreased the CAC of the block oligomers. Table 2 and Figure 3 show that a 10- to 60-fold reduction of the CAC is obtained by benzoylation. The effect of naphthoylation is even larger, indicated for example by the 200-fold reduction of the CAC of mPEG750-*b*-$OCL_4$, measured with 1,8-ANS. It is noteworthy that these low CAC values are even comparable to those of high molecular weight PEG-*b*-PCL, which have already been used for the delivery of cyclosporine A in vivo.[47] Remarkably, the CAC values found with the pyrene and the 1,8-ANS method leveled off at the lowest values of 0.003 and 0.01 mg/mL, respectively, suggesting that we reached the detection limits of the methods. In literature, values lower than 0.001 mg/mL (pyrene method) were rarely reported either. Calculations based on partition equilibrium coefficients of pyrene and the volume fraction of the hydrophobic core of the micelles[34] indeed suggest that the total amount of pyrene in water and inside the hydrophobic core of the micelles is almost equal at the lowest amphiphile concentration. Since 1,8-ANS is more hydrophilic, it has a lower partition equilibrium coefficient, which explains the lower sensitivity of the method (0.01 mg/mL). This means that the effect of end group modification on the CAC may be even larger than suggested by the reported data.

**Self-Assembly of mPEG-*b*-oligocaprolactones with and without End Group Modification.** After the particle formation by hydration of an oligomer film with PBS, followed by filtration, a block oligomer recovery of >90% was found with analytical GPC. This indicates that hardly any material was lost during the process. Dynamic light scattering (DLS) measurements demonstrated that the block oligomers with a relatively large PEG fraction formed nanoparticles with a hydrodynamic diameter ($Z_{ave}$) of 30−200 nm (Figure 4), and a relatively high polydispersity index (PDI) of 0.2−0.6, which was observed previously for mPEG-*b*-oligolactates as well.[35] Interestingly, mPEG750-*b*-OCL with a DP larger than 4 forms small, almost monodisperse nanoparticles (PDI < 0.1) with a diameter smaller than 15 nm (Figure 4). With the benzoylated and naphthoylated block oligomers, these small particles are even obtained at an OCL DP of 2 and higher. Our data suggest that a CAC lower than 1.5 mg/mL (determined with 1,8-ANS, see Table 2) favors the formation of sub-20-nm particles. Figure 4 demonstrates a growth in the particle diameter with increasing length of the hydrophobic block. The increase in diameter per caprolactone unit measures 1.4 nm, and benzoylation and naphthoylation result in an increase of 4 and 5 nm, respectively. Taking this into account, as well as the particle size in relation to the end-to-end distance of the block oligomers, the formed nanoparticles likely have a micellar morphology. For example, the end-to-end distance of a fully stretched mPEG750-*b*-$OCL_6$ chain is 11 nm, resulting in a theoretical micellar diameter of 22 nm. This is in reasonable agreement with the measured particle diameter of 9.3 nm, in which the oligomer chains will be at least partly coiled rather than fully stretched. Similarly, the length of a caprolactone unit (1 nm) in corresponds well with the size increase. The effect of end group modification on the diameter is larger than the size of the benzoyl- or naphthoyl group (0.6 and 0.9 nm, respectively), likely because of a different packing

**Table 2. Critical Aggregation Concentration of (Modified) mPEG-*b*-OCL in PBS**

| | mPEG750-*b*-$OCL_x$ | | benzoylated mPEG750-*b*-$OCL_x$ | | naphthoylated mPEG-*b*-$OCL_x$ | |
|---|---|---|---|---|---|---|
| *x* | CAC ANS (mg/mL)[a] | CAC pyrene (mg/mL)[b] | CAC ANS (mg/mL)[a] | CAC pyrene (mg/mL)[b] | CAC ANS (mg/mL)[a] | CAC pyrene (mg/mL)[b] |
| 1 | NA[e] | NA[e] | 5.1 | 0.50 | 0.38[c] | ND[d] |
| 2 | >10 | 3.4 | 1.2 | 0.42 | 0.18 | ND[d] |
| 3 | >10 | 1.5 | 0.43 | 0.10 | 0.05 | ND[d] |
| 4 | 4.4 | 1.0 | 0.04 | 0.034 | 0.02 | ND[d] |
| 5 | 1.1 | 0.52 | 0.01 | 0.008 | 0.01 | ND[d] |
| 6 | 0.26 | 0.17 | 0.01 | 0.003 | 0.01 | ND[d] |
| 7 | 0.09 | 0.03 | 0.01 | 0.003 | NA[e] | NA[e] |

[a] The standard error of the method was 10−15%. [b] The standard error of the method was 5−10%. [c] This value may be slightly lower than the real CAC, as a result of the fluorescence of the naphthoyl end group: in the control samples (without 1,8-ANS), fluorescence is observed at block oligomer concentrations of 0.3 mg/mL and higher. [d] Not detectable; the fluorescence of the naphthoyl end group interfered with the fluorescence of pyrene. [e] NA = Not available

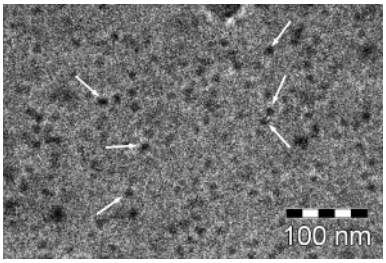


**Figure 5.** Cryo-TEM image of benzoylated mPEG750-*b*-$OCL_6$ particles at 10 mg/mL in phosphate buffered saline. Some of the nanoparticles are indicated by white arrows. The diameter of the nanoparticles is approximately 10 nm.

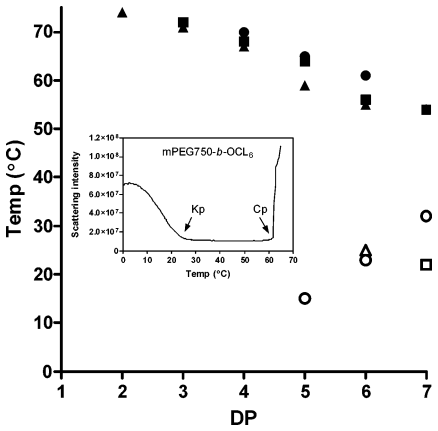


**Figure 6.** Krafft points (Kp, open symbols) and cloud points (Cp, closed symbols) of mPEG750-*b*-$OCL_x$ (circles), benzoylated mPEG750-*b*-$OCL_x$ (squares), and naphthoylated mPEG750-*b*-$OCL_x$ (triangles). Note: The block oligomers with an OCL DP < 5 (unmodified), < 7 (benzoylated), and < 6 (naphthoylated) do not display a Kp above 0 °C.

in the hydrophobic core, caused by the aromatic groups. The spherical shape of these small nanoparticles was confirmed by cryo-TEM. Figure 5 shows a picture of nanoparticles composed of benzoylated mPEG750-*b*-$OCL_6$ in PBS, which have a diameter of approximately 10 nm.

**Thermosensitivity and Stability of the Block Oligomer Dispersions.** When heating a dispersion of mPEG750-*b*-OCL with a DP greater than 5, first a decrease in static light scattering was observed, reflecting the Krafft point (Kp) (Figure 6). The Kp represents the temperature at which the solubility of an amphiphilic polymer equals the CAC. Below the Kp the amphiphiles are precipitated, because the solubility is not sufficient to form micelles, whereas above the Kp the concentration of dissolved amphiphiles is high enough to favor the self-assembly into micelles. As expected, the Kp increased from <0 °C (for DP 2−4) to 32 °C when the DP of the OCL block increased from 2 to 7 units (Figure 6). Similar behavior was observed by Letchford et al., who reported Kp's of 27, 30, and 31 °C for polydisperse mPEG750-*b*-OCLs, with an average OCL chain length of 2, 5, and 10 units, respectively.[34] Interestingly, the observed Kp's of the fractionated, unmodified mPEG750-*b*-OCLs are slightly above the onset of the melting endotherms of the OCL block (see DSC of MEE−OCL, Figure 2a). This suggests that melting of the hydrophobic block increases the aqueous solubility of the block oligomer, and when the solubility reaches the CAC, the Kp is observed. Figure 7a shows a schematic representation of the block oligomer concentration in water (either molecularly dissolved or as micelles) vs temperature, illustrating the relation between the DP, the $T_m$, the solubility, the CAC and the Kp. With increasing DP, the

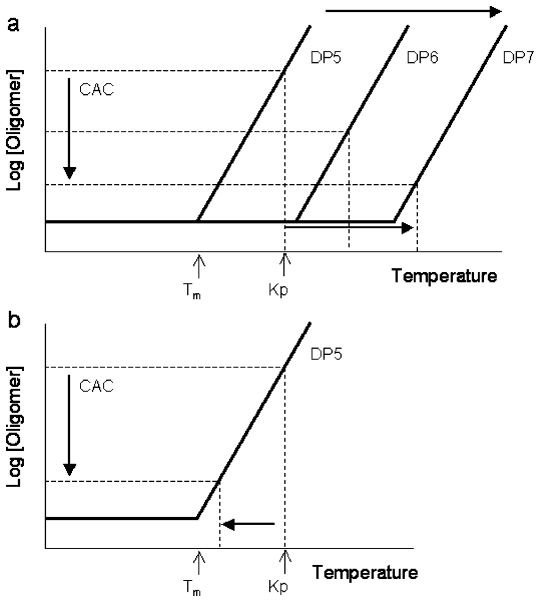


**Figure 7.** Schematic representation of the relation between the melting temperature ($T_m$), the solubility (log[oligomer], i.e. concentration of oligomer that is molecularly dissolved or present as micelles), the critical aggregation concentration (CAC) and the Krafft point (Kp), and the effect of the DP (a) and end group modification (b) thereon.

onset of dissolution (represented by the inflection point of the curves) shifts to higher temperatures, because of an increased $T_m$ of the hydrophobic block. Therefore, the Kp increases with increasing DP, as reflected by the horizontal arrow in Figure 7a, even though the CAC decreases with increasing DP. Surprisingly, the effect of the end group modification on the Kp is opposite to the effect of increasing DP: the modified mPEG-*b*-OCLs had a lower Kp (<0−25 °C) than their unmodified counterparts (Figure 6). This peculiar behavior can be explained with the help of Figure 7b. As mentioned before, end group modification hardly affects the thermal behavior of the block oligomers, and therefore the onset of dissolution is not changed. However, the CAC is greatly reduced (Table 2), which causes a reduction of the Kp, as illustrated by the arrows in Figure 7b.

Further heating of the dispersions resulted in the occurrence of a cloud point (Cp) in the dispersions of monodisperse mPEG750-*b*-OCL with a DP greater than 3 (Figure 6). The Cp is ascribed to the dehydration of the PEG part of the block oligomers, causing aggregation of the self-assembled particles, which is reflected by an increase in turbidity. As expected, the Cp's decreased with increasing DP of the OCL block, and the introduction of an aromatic group caused a decrease in the Cp's as well (Figure 6). Similar observations were described for polydisperse PEG-*b*-OCL,[34] PEG-*b*-polycaprolactone-*co*-trimethylene carbonate (PCL-*co*-TMC)[48] and low molecular weight nonionic surfactants.[49] Preferably, the thermosensitivity of amphiphiles used for drug delivery purposes should not interfere with their application at body temperature, nor with handling or storage at room temperature or 4 °C. This is illustrated by the low stability of the micelles composed of mPEG750-*b*-$OCL_6$, benzoylated mPEG750-*b*-$OCL_7$, and naphthoylated mPEG750-*b*-$OCL_6$, which precipitated within approximately 2 weeks, and of mPEG750-*b*-$OCL_7$, which precipitated within 1 h, when stored at room temperature (results not shown). This is likely due to the presence of their Krafft point close to or below the storage temperature (Figure 6). The oligomeric micelles formed by the other modified and unmodified mPEG-*b*-OCLs in PBS retained their small size for over a month when stored

at room temperature, and for at least 2 weeks when incubated at 37 °C (results not shown).

## Conclusions

This study demonstrates that end group modified mPEG-*b*-oligocaprolactones with monodisperse hydrophobic blocks are very interesting amphiphiles for drug delivery purposes. They self-assemble into micelles with a diameter smaller than 15 nm, which may have attractive properties in terms of biodistribution and tissue penetration in vivo. Furthermore, end group modification with an aromatic group substantially decreased the CAC of the mPEG-*b*-OCLs, which even approached those of high molecular weight mPEG-*b*-PCL. This interesting observation will confer these micelles a higher stability toward dilution upon administration and longer retention of the loaded drug. These aspects will be the subject of future work to evaluate the pharmaceutical applicability of these oligomeric micelles.

**Acknowledgment.** This research was financially supported by OctoPlus N.V., Leiden, The Netherlands.

## References and Notes

(1) Kabanov, A. V.; Batrakova, E. V.; Melik-Nubarov, N. S.; Fedoseev, N. A.; Dorodnich, T. Y.; Alakhov, V. Y.; Chekhonin, V. P.; Nazarova, I. R.; Kabanov, V. A. *J. Controlled Release* **1992**, *22*, 141−157.
(2) Kwon, G. S.; Yokoyama, M.; Okano, T.; Sakurai, Y.; Kataoka, K. *Pharm. Res.* **1993**, *10*, 970−974.
(3) Allen, C.; Maysinger, D.; Eisenberg, A. *Colloids Surf. B* **1999**, *16*, 3−27.
(4) Gaucher, G.; Dufresne, M. H.; Sant, V. P.; Kang, N.; Maysinger, D.; Leroux, J. C. *J. Controlled Release* **2005**, *109*, 169−188.
(5) Maeda, H.; Wu, J.; Sawa, T.; Matsumura, Y.; Hori, K. *J. Controlled Release* **2000**, *65*, 271−284.
(6) Edlund, U.; Albertsson, A. C. *Adv. Drug Delivery Rev.* **2003**, *55*, 585−609.
(7) Albertsson, A. C.; K. Varma, I. *Biomacromolecules* **2003**, *4*, 1446−1486.
(8) Sinha, V. R.; Bansal, K.; Kaushik, R.; Kumria, R.; Trehan, A. *Int. J. Pharm.* **2004**, *278*, 1−23.
(9) Woodle, M. C.; Lasic, D. D. *Biochim. Biophys. Acta* **1992**, *1113*, 171−199.
(10) Storm, G.; Belliot, S. O.; Daemen, T.; Lasic, D. D. *Adv. Drug Delivery Rev.* **1995**, *17*, 31−48.
(11) Torchilin, V. P.; Trubetskoy, V. S. *Adv. Drug Delivery Rev.* **1995**, *16*, 141−155.
(12) Gref, R.; Domb, A.; Quellec, P.; Blunk, T.; Muller, R. H.; Verbavatz, J. M.; Langer, R. *Adv. Drug Delivery Rev.* **1995**, *16*, 215−233.
(13) Burt, H. M.; Zhang, X.; Toleikis, P.; Embree, L.; Hunter, W. L. *Colloids Surf., B* **1999**, *16*, 161−171.
(14) Govender, T.; Riley, T.; Ehtezazi, T.; Garnett, M. C.; Stolnik, S.; Illum, L.; Davis, S. S. *Int. J. Pharm.* **2000**, *199*, 95−110.
(15) Peracchia, M. T.; Gref, R.; Minamitake, Y.; Domb, A.; Lotan, N.; Langer, R. *J. Controlled Release* **1997**, *46*, 223−231.
(16) Shuai, X.; Ai, H.; Nasongkla, N.; Kim, S.; Gao, J. *J. Controlled Release* **2004**, *98*, 415−426.
(17) Kim, S. Y.; Lee, Y. M. *Biomaterials* **2001**, *22*, 1697−1704.
(18) Forrest, M. L.; Won, C. Y.; Malick, A. W.; Kwon, G. S. *J. Controlled Release* **2005**, *110*, 370−377.
(19) Aliabadi, H. M.; Mahmud, A.; Sharifabadi, A. D.; Lavasanifar, A. *J. Controlled Release* **2005**, *104*, 301−311.
(20) Lim Soo, P.; Lovric, J.; Davidson, P.; Maysinger, D.; Eisenberg, A. *Mol. Pharm.* **2005**, *2*, 519−527.
(21) Vonarbourg, A.; Passirani, C.; Saulnier, P.; Benoit, J. P. *Biomaterials* **2006**, *27*, 4356−4373.
(22) Sun, X.; Rossin, R.; Turner, J. L.; Becker, M. L.; Joralemon, M. J.; Welch, M. J.; Wooley, K. L. *Biomacromolecules* **2005**, *6*, 2541−2554.
(23) Weissig, V.; Whiteman, K. R.; Torchilin, V. P. *Pharm. Res.* **1998**, *15*, 1552−1556.
(24) Rosler, A.; Vandermeulen, G. W.; Klok, H. A. *Adv. Drug Delivery Rev.* **2001**, *53*, 95−108.
(25) Rodriguez-Hernandez, J.; Checot, F.; Gnanou, Y.; Lecommandoux, S. *Prog. Polym. Sci.* **2005**, *30*, 691−724.
(26) Shuai, X.; Merdan, T.; Schaper, A. K.; Xi, F.; Kissel, T. *Bioconjugate Chem.* **2004**, *15*, 441−448.
(27) Yokoyama, M.; Opanasopit, P.; Okano, T.; Kawano, K.; Maitani, Y. *J. Drug Targeting* **2004**, *12*, 373−384.
(28) Opanasopit, P.; Yokoyama, M.; Watanabe, M.; Kawano, K.; Maitani, Y.; Okano, T. *Pharm. Res.* **2004**, *21*, 2001−2008.
(29) Watanabe, M.; Kawano, K.; Yokoyama, M.; Opanasopit, P.; Okano, T.; Maitani, Y. *Int. J. Pharm.* **2006**, *308*, 183−189.
(30) Kabanov, A. V.; Batrakova, E. V.; Alakhov, V. Y. *J. Controlled Release* **2002**, *82*, 189−212.
(31) Harada, A.; Kataoka, K. *Science* **1999**, *283*, 65−67.
(32) Yoshida, E.; Kunugi, S. *J. Polym. Sci., Part A: Polym. Chem.* **2002**, *40*, 3063−3067.
(33) Kang, N.; Perron, M.-E.; Prud'homme, R. E.; Zhang, Y.; Gaucher, G.; Leroux, J.-C. *Nano Lett.* **2005**.
(34) Letchford, K.; Zastre, J.; Liggins, R.; Burt, H. *Colloids Surf., B* **2004**, *35*, 81−91.
(35) Carstens, M. G.; van Nostrum, C. F.; Ramzi, A.; Meeldijk, J. D.; Verrijk, R.; de Leede, L. L.; Crommelin, D. J. A.; Hennink, W. E. *Langmuir* **2005**, *21*, 11446−11454.
(36) Soga, O.; van Nostrum, C. F.; Ramzi, A.; Visser, T.; Soulimani, F.; Frederik, P. M.; Bomans, P. H. H.; Hennink, W. E. *Langmuir* **2004**, *20*, 9388−9395.
(37) Nakahara, Y.; Kida, T.; Nakatsuji, Y.; Akashi, M. *Langmuir* **2005**, *21*, 6688−6695.
(38) Walter, A.; Kuehl, G.; Barnes, K.; VanderWaerdt, G. *Biochim. Biophys. Acta* **2000**, *1508*, 20−33.
(39) Abuin, E. B.; Lissi, E. A.; Aspee, A.; Gonzalez, F. D.; Varas, J. M. *J. Colloid Interface Sci.* **1997**, *186*, 332−338.
(40) Priev, A.; Zalipsky, S.; Cohen, R.; Barenholz, Y. *Langmuir* **2002**, *18*, 612−617.
(41) Penco, M.; Sartore, L.; Bignotti, F.; D'Antone, S.; Di Landro, L. *Eur. Polym. J.* **2000**, *36*, 901−908.
(42) Cerrai, P.; Tricoli, M.; Andruzzi, F.; Paci, M.; Paci, M. *Polymer* **1989**, *30*, 338−343.
(43) Sosnik, A.; Cohn, D. *Polymer* **2003**, *44*, 7033−7042.
(44) He, C.; Sun, J.; Zhao, T.; Hong, Z.; Zhuang, X.; Chen, X.; Jing, X. *Biomacromolecules* **2005**.
(45) Sun, J.; Chen, X.; He, C.; Jing, X. *Macromolecules* **2006**.
(46) Van Alstine, J. M.; Sharp, K. A.; Brooks, D. E. *Colloids Surf.* **1986**, *17*, 115−121.
(47) Aliabadi, H. M.; Brocks, D. R.; Lavasanifar, A. *Biomaterials* **2005**, *26*, 7251−7259.
(48) Ould-Ouali, L.; Arien, A.; Rosenblatt, J.; Nathan, A.; Twaddle, P.; Matalenas, T.; Borgia, M.; Arnold, S.; Leroy, D.; Dinguizli, M.; Rouxhet, L.; Brewster, M.; Preat, V. *Pharm. Res.* **2004**, *21*, 1581−1590.
(49) Schott, H. *J. Pharm. Sci.* **1969**, *58*, 1443−1449.

MA0619738